ISSN 1063-7850, Technical Physics Letters, 2016, Vol. 42, No. 4, pp. 395–398. © Pleiades Publishing, Ltd., 2016.
Original Russian Text © M.E. Pinchuk, A.V. Budin, I.I. Kumkova, A.N. Chusov, 2016, published in Pis'ma v Zhurnal Tekhnicheskoi Fiziki, 2016, Vol. 42, No. 8, pp. 10–17.

Studying Energy Evolution in the Discharge Chamber of a Multichamber Lightning Protection System

M. E. Pinchuk[a]*, A. V. Budin[a], I. I. Kumkova[a], and A. N. Chusov[b]

[a] *Institute for Electrophysics and Electric Power, Russian Academy of Sciences, St. Petersburg, 191186 Russia*

[b] *Streamer Electric Inc., St. Petersburg, 191024 Russia*

**e-mail: pinchme@mail.ru*

Received November 17, 2015

Abstract—We present experimental data on the distribution of energy deposition along the discharge chamber of a multichamber lightning protection system at the initial stage of a discharge process modeling a lightning current pulse with 10 kA amplitude. The multichamber system comprised serially connected gas-discharge chambers. The breakdown between electrodes situated on the bottom of a channel in each chamber induces the formation of a shock wave. Subsequent energy evolution during the development of discharge proceeds in the entire volume bounded by the shock wave.

DOI: 10.1134/S1063785016040222

Aerial power transmission lines are protected from lightning-induced surges by complexes of special devices [1–3]. The main elements of these complexes are overhead ground-wire systems [1–3], overvoltage limiters based on nonlinear resistors [2], and gas-discharge gaps of various types [2, 3]. Protective devices of all types are being continuously improved [2–4], their elements are being modified, and new approaches to protecting power transmission lines against lightning are being developed [3, 4].

Modern surge protective gas-discharge gaps employ discharges of various types [3, 5–9]. New methods of limiting overvoltages in power transmission lines have been recently developed [3, 5–9], in particular, based on controlled gas-discharge triggering systems [5–7]. The most promising surge suppressing elements for lightning protection systems include multichamber discharge gaps developed at the Streamer Electric Inc. (St. Petersburg, Russia) [10], taking the form of serially connected two-electrode discharge chambers embedded into a profiled silicon rubber matrix [3, 8, 9].

The performance characteristics of these devices obey all modern requirements to lightning protection [11], and the Streamer products are frequently preferred in designing and constructing new power transmission lines [3, 10].

This Letter presents experimental data on the distribution of energy deposition along a discharge chamber of the multichamber lightning protection system [9]. The development of new lightning protection systems is a difficult and expensive task. To optimize the approach to designing these systems, there have been attempts to formulate physico-mathematical models of discharge and calculate the parameters of a medium in discharge chambers [12, 13]. The present investigation was inspired by discrepancies between the results of modeling [13] and theoretical estimations [14] of the parameters of gas flow and the experimental data [14]. Indeed, the calculated values [13, 14] of the shock wave propagation velocities are much lower than those observed in experiment [14].

When lightning strikes an aerial power transmission line, sequential breakdowns take place in discharge gaps between electrodes situated on the bottom of a channel in each discharge chamber serially connected into a multichamber lightning protection system. The shock wave formed at the breakdown stage pushes a significant amount of gas out from the discharge chamber. After the passage of a current pulse and the reduction of pressure in the discharge volume, external air refills the discharge chamber. The rate of deionization of the discharge gap is determined by the rate of refilling and, hence, depends on the amount of gas pushed out by the shock wave. Thus, parameters of the shock wave and gas flow at the initial stage of discharge determine to a large degree the performance characteristics of the multichamber lightning protection system and its ability to quench the accompanying current passage from the power transmission line.

The experiments were carried out in a setup described in detail elsewhere [15]. The methods of discharge plasma diagnostics were recently briefly reviewed in [16]. In this work, we have studied the profile of energy deposition in a single discharge chamber of the multichamber lightning protection system [9].

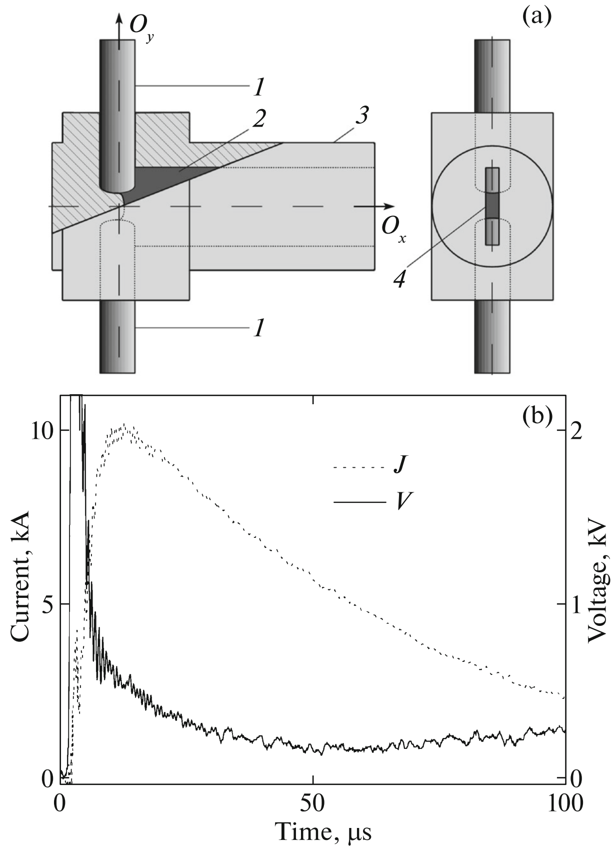

Fig. 1. (a) Schematic diagram of one discharge chamber of the multichamber lightning protection system: (*1*) electrode, (*2*) discharge volume, (*3*) discharge chamber case, and (*4*) output cross section of the discharge gap. (b) Typical waveforms of the discharge current (*J*) and voltage (*V*).

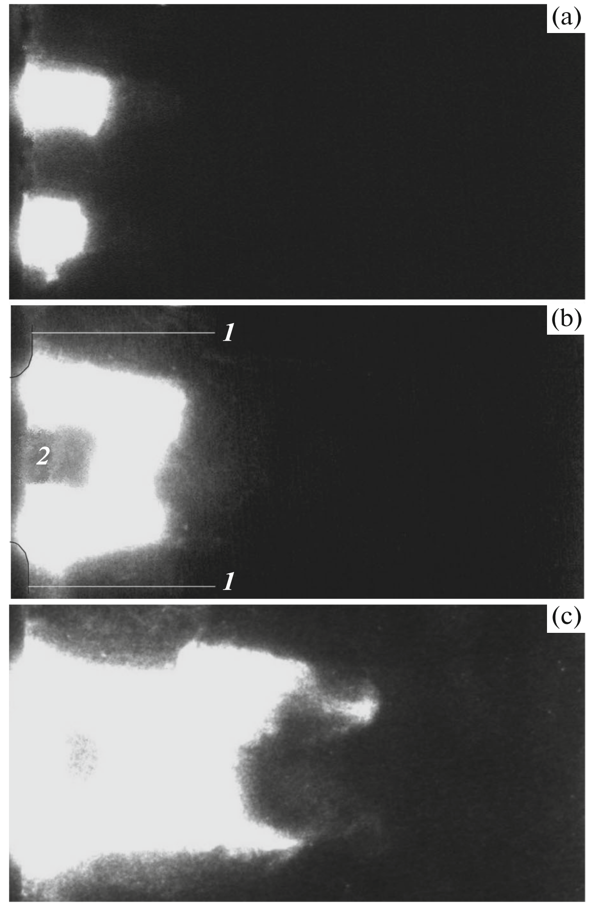

Fig. 2. High-speed video recording frames of discharge channel at the time moments (a) 3 μs, (b) 5 μs, and (c) 10 μs after discharge initiation: (*1*) electrode contour; (*2*) dielectric protrusion on the bottom of discharge volume.

Figure 1a shows a schematic diagram of one discharge chamber of the multichamber lightning protection system under consideration. The model chamber was made of a silicon rubber. The discharge volume represents a 2-cm-long narrow gap with rectangular cross section (1 cm high, 0.1 cm wide), which is open to atmosphere at one end. Figure 1b shows the current and voltage waveforms measured in the discharge gap. A current pulse with an amplitude of 10 kA and an initial ramp of ~10^9 A/s was generated using a ~30 μF capacitor charged at a voltage of 18–23 kV and discharged to a single discharge chamber via a 2 Ω resistor. Thus, the current amplitude was determined by this resistor, the time constant of the discharge circuit was ~60 μs, and the energy deposited in discharge was ~200 J.

Figure 2 shows a series of three frames from a high-speed video recording in the side projection of discharge development, each measured with a 15-ns exposure at the time moments 3, 5, and 10 μs after discharge initiation. For video recording in the side projection, the discharge chamber case was cut out up to the boundary of discharge gap and the wall was replaced by a rigidly fixed plate of transparent polycarbonate. Using a discharge gap of planar geometry, it is possible to reconstruct the field of energy evolution in the discharge volume from the data of high-speed video recording.

In the object under consideration, the gas medium density was $\rho \sim 1.2$ kg/m^3, the characteristic size of jet flow was $L \sim 2 \times 10^{-2}$ m, the flow cross-section area was $S \sim 10^{-5}$ m^2, and the characteristic energy deposited at the initial stage was within $W_{in} \sim 10$–25 J. After breakdown of the interelectrode gap and subsequent formation of the discharge channel, energy $W_{in} \sim 10$–25 J is deposited within several microseconds in a relatively small region, so that a shock-wave front is generated.

For mass $m \sim 0.25$ mg of gas in the discharge chamber, the deposition of energy W_{in} into this whole amount changes the gas pressure and temperature to $p \sim 7$–15 MPa and $T \sim 10\,000$–20 000 K. The velocity of sound in this medium is $c \sim 2.5$–4 km/s. Under these conditions, discharge plasma can be consid-

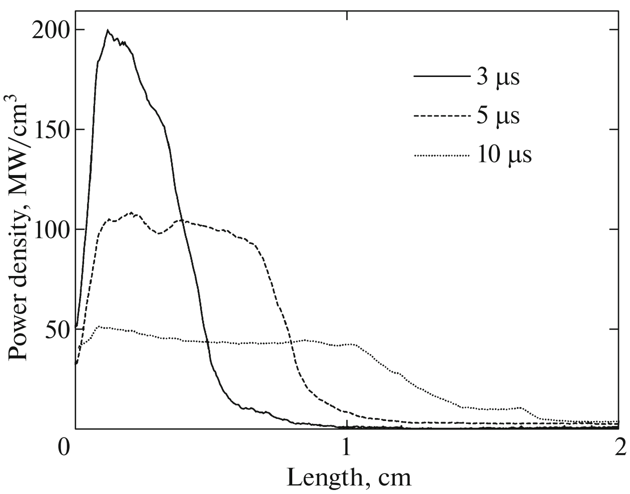

Fig. 3. Profiles of energy deposition along discharge chamber axis *Ox* at the time moments 3, 5, and 10 μs after discharge initiation.

ered transparent, at least during an early stage prior to mass supply of the chamber wall material to the discharge volume at relatively small current densities (~10^4 A/cm^2).

The average gas efflux velocity (at an efficiency of $\chi \sim 0.5$) can be estimated from the relation

$$\rho SL\frac{v^2}{2} \sim \chi W_{\rm in}$$

which yields

$$v \sim 0.5\left(\frac{2\chi W_{\rm in}}{pSL}\right)^{1/2} 3-7 \text{ km/s}.$$

The characteristic times of heat transfer can be estimated as $L^2/4a \sim 0.1$ s and $l^2/4a \sim 250$ μs, where $a \sim 10^{-3}$ m^2/s is the thermal diffusivity of air and $l \sim 10^{-3}$ m is the size of the wave front. Thus, it can be suggested that heat is transferred together with the gas flow and transport phenomena can be ignored.

High-speed video recording was carried out in a relatively narrow spectral interval of 550–650 nm limited by optical filters. For the above estimation of plasma temperature, the spectral emissivity in this spectral interval is directly proportional to the temperature as $I_\lambda \sim T$ [17]. Then, assuming that local energy evolution at a given point is spent on increasing the temperature (to within the kinetic energy of the gas), we conclude that the obtained optical image reflects the field of energy deposition in the discharge volume with a flat geometry as

$$P(t) = J(t)V(t) = \iint P_{xy}(x,y,t)dxdy\Delta z$$
$$\sim \iint I_\lambda(x,y,t)dxdy,$$

where $P(t)$ is the power deposited in discharge, $J(t)$ is the discharge current, $V(t)$ is the voltage drop on the discharge gap, $P_{xy}(x, y, t)$ is the spatial distribution of specific power in the flat geometry, Δz is the discharge gap width, and $I_\lambda(x, y, t)$ is the field of emission intensity from the discharge gap at a given moment of time. In fact, $I_\lambda(x, y, t)$ field corresponds to the distribution of emission intensity on the high-speed video recording at this moment of time.

Using the images obtained by high-speed video recording, it is possible to reconstruct two-dimensional fields of energy evolution in the discharge volume. However, in the given case, a more illustrative pattern is provided by one-dimensional profiles of energy deposition $P_x(x, t)$ along discharge axis *Ox* (Fig. 3):

$$P_x(x,t) \sim \int I_\lambda(x,y,t)dy.$$

As can be seen from Fig. 3, energy deposition during discharge development takes place over the entire volume limited by the shock wave. High-speed video recording in the side projection of discharge development shows that the emission field occupies the entire space from the discharge chamber bottom up to the propagating shock-wave front.

Therefore, the propagating shock wave obtains additional energy from discharge. This conclusion confirms the suggestions made in [14]. The data presented above can be used in the formulation and correction of physico-mathematical models of discharge in analogous surge protection systems.

Acknowledgments. This work was performed in the framework of the program "Research and Development in High-Priority Directions of the Science and Technology Complex in Russia for 2014–2020," project no. 14.579.21.0041 of August 21, 2014 (unique project identifier code: RFMEF157914X0041).

REFERENCES

1. T. M. Bazelyan and Y. P. Raizer, *Lightning Physics and Lightning Protection* (Nauka, Moscow, 2001; IOP, Bristol, 2000).
2. G. N. Aleksandrov, *Lightning and Lightning Protection* (Nauka, Moscow, 2008) [in Russian].
3. G. V. Podporkin, *Lightning Protection of Aerial Power Lines* (Rodnaya Ladoga, St. Petersburg, 2015) [in Russian].
4. A. V. Kolychev, Yu. S. Popova, and F. Kh. Khalilov, ELEKTRO: Elektrotekh. Elektroenerg. Elektrotekh. Prom-st, No. 5, 20 (2009).
5. Yao Xueling, Chen Jingliang, Xu Xiaowei, Liu Yong, and Zhao Yong, Plasma Sci. Technol. **12** (1), 113 (2010).
6. W. Sun, Y. Li, D. Lu, X. Zhao, and Y. Yu, Adv. Mater. Res. **368–373**, 3344 (2012).
7. Yao Xueling and Chen Jingliang, Plasma Sci. Technol. **14**, 759 (2012).

8. G. V. Podporkin, E. Yu. En'kin, and V. E. Pil'shchikov, Elektrotekhnika, No. 1, 2 (2013).
9. G. V. Podporkin, E. Yu. En'kin, and V. E. Pil'shchikov, Elektrichestvo, No 1, 26 (2013).
10. http://www.streamer.ru/; map of installed devices: http://map.streamer.ru/
11. IEC61024 (1990). Protection of structures against lightning. Part 1: General Principles. International Electrotechnical Commission (IEC) Std.
12. V. Ya. Frolov, D. V. Ivanov, Yu. V. Murashov, and A. D. Sivaev, Tech. Phys. Lett. **41** (4), 310 (2015).
13. Guo Zhiwei, Long Xinping, Qian Zhongdong, and Qiu Ning, Private communication (2016).
14. A. V. Glushneva, A. S. Saveliev, E. E. Son, and D. V. Tereshonok, Tech. Phys. **60** (3), 471 (2015).
15. M. E. Pinchuk, A. V. Budin, V. E. Pil'shchikov, A. G. Leks, and V. V. Leont'ev, Instr. Exp. Tech. (2016) [in press].
16. M. E. Pinchuk, A. A. Bogomaz, A. V. Budin, and P. G. Rutberg, IEEE Trans. Plasma Sci. **42** (10), 2434 (2014).
17. Ya. B. Zeldovich and Yu. P. Raizer, *Physics of Shock Waves and High-Temperature Hydrodynamic Phenomena* (Nauka, Moscow, 1966) [in Russian].

Translated by P. Pozdeev